Supporting Information

Inorganic-Organic Hybrid Fluorescent Binary Probe for DNA Detection Based on Spin-Forbidden Resonance Energy Transfer

Angel A. Martí,[†] Cindy A. Puckett,[‡] Joanne Dyer,[†,§] Nathan Stevens,[†] Steffen Jockusch,[†] Jingyue Ju,[∥,⊥] Jacqueline K. Barton,[‡] Nicholas J. Turro[†,⊥,*]

[†]*Department of Chemistry and* [⊥]*Department of Chemical Engineering Columbia University, New York, NY 10027.* [‡]*Division of Chemistry and Chemical Engineering, California Institute of Technology, Pasadena, California 91125.* [∥]*Columbia Genome Center, Columbia University College of Physicians and Surgeons, New York, NY 10032.*

Experimental procedure

Probe sequence

The probe sequences are complementary to a region of *Aplysia californica* sensorin mRNA. A region low in secondary structure was selected as the target for the binary probe based on the modeled secondary structure. The modeling details have been reported elsewhere.[1]

Ru-probe: 5'-AAG TTG ATC AAG TTG GT-(Ru(bpy')$(DIP)_2^{2+}$)-3'
Alexa-Probe: 5'-AAG TTG ATC AAG TTG GT-(Alexa488)-3'
Cy5-Probe-1: 5'-Cy5-TAT GTT TCA CTG GAT GA-3'
Cy5-Probe-2: 5'-Cy5-ATG TTT CAC TGG ATG A-3'
Cy5-Probe-3: 5'-Cy5-TTC ACT GGA TGA-3'
Target: 5'-TCA TCC AGT GAA ACA TAC AGC ACC AAC TTG ATC AAC TT-3'

Probe Systems
PS1: Ru-Probe + Cy5-Probe-1
PS2: Ru-Probe + Cy5-Probe-2
PS3: Ru-Probe + Cy5-Probe-3
PS4: Alexa-Probe + Cy5-Probe-3

Probe synthesis

$[Ru(DIP)_2bpy']Cl_2$. $Ru(DIP)_2Cl_2$ was synthesized in analogous fashion to the published synthesis of $Ru(bpy)_2Cl_2$.[2] $Ru(DIP)_2bpy'^{2+}$ was prepared by refluxing 41 mg of $Ru(DIP)_2Cl_2$ (49 μmol) and 16.4 mg (64 μmol) of 4-(3-carboxypropyl)-4'-methyl-2,2'-bipyridine (prepared according to the published procedure[3]) in 10 mL of 1-1 ethanol/water for 3 h. The mixture was cooled to room temperature and the ethanol removed in vacuo. The solution was diluted with water (20 mL) and filtered. The complex was precipitated as the PF_6^- salt by addition of NH_4PF_6, then returned to the Cl^- salt using a Sephadex DEAE anion exchange column. ESI-MS: m/z = 511.

Ru-probe. $Ru(DIP)_2bpy'^{2+}$ was tethered to the 3'-end of DNA by first coupling the complex to amine-modified beads, followed by DNA synthesis and cleavage of the Ru-

DNA conjugate from the beads.[4] The FMOC group was removed from 3'-amino-modifier C7 CPG 500 beads (Glen Research) by incubation with 20% piperidine in DMF for 15 min. The beads were rinsed with DMF and CH_3CN, dried in vacuo, then placed under Ar. To the beads (2 μmol), $[Ru(DIP)_2bpy']Cl_2$ (4.5 mg, 4 μmol), HBTU (1.5 mg, 4 μmol), HOBT (0.6 mg, 4 μmol), and DIEA (2 μL, 12 μmol) in anhydrous DMF (1.5 mL) were added. The reaction mixture was shaken for 30 min. at room temperature. The beads were rinsed with DMF, CH_3CN, and CH_2Cl_2, then divided into two aliquots and transferred into two DNA synthesis columns. DNA was synthesized using an ABI 3400 DNA synthesizer. The DNA was cleaved from the beads and deprotected with conc. NH_4OH (2 h at RT, 6 h at 60 °C). The Ru-DNA conjugate was purified by HPLC using a gradient of 5:95 to 65:35 (acetonitrile/50 mM ammonium acetate) over 30 min. The DMT was removed with 80% acetic acid for 15 min. at room temperature, followed by addition of ethanol, and removal of solvent in vacuo. The Ru-DNA conjugate was purified once more by HPLC. MALDI-TOF: 6473 (obs'd), 6477 (calc'd).

Cy5-probes. DNA was synthesized using 'ultramild' reagents with Cy5 was added at the 5'-end, using a Cy5 phosphoramidite (Glen Research). The MMT group was removed by the DNA synthesizer. The DNA was cleaved and deprotected with 0.05 M potassium carbonate in methanol for 4 h at room temperature. To the supernatant, 1.5 equivalents by volume 2 M TEAA was added. The solution was concentrated in vacuo and desalted using a Nap10 column (GE Healthcare), eluting with water. The Cy5-DNA conjugate was purified by HPLC using a gradient of 5:95 to 65:35 (acetonitrile/50 mM ammonium acetate) over 30 min. MALDI-TOF: Cy5-Probe-1, 5748 (obs'd), 5749 (calc'd); Cy5-Probe-2, 5442 (obs'd), 5445 (calc'd); Cy5-Probe-3, 4193 (obs'd), 4194 (calc'd).

Steady-state and time-resolved luminescence experiments

Steady-state luminescence spectra were performed on a FL3-22 Fluorolog-3 spectrometer (J. Y. Horiba, Edison, NJ, USA) in quartz cuvettes of 0.4 mm path length. In a typical experiment, the spectra were obtained in solutions of 0.5 μM Ru-probe and 0.5 μM Cy5-probe in 250 μL of 10 mM Tris-HCl, 400 mM NaCl, 5mM $MgCl_2$ pH 7.5. Target was added in 1:1 proportion (probes:target) to a final target concentration of 0.5 μM. The experiments using Alexa-Cy5 system (PS4) were performed similarly and the details are reported elsewhere.[5] The steady-state spectra were corrected for spectral efficiencies of the monochromator and PMT.

Time-resolved experiments were performed on an OB920 single-photon counting spectrometer (Edinburgh Analytical Instruments) with a Picoquant 460 nm pulsed LED or 659 nm diode laser as excitation source. Exponential fits were obtained with a program included with the instrument (F900, v6.42). Iterative reconvolution with the instrument response function (IRF) was employed for Cy5 decays, using a time window of 20 ns. Lifetimes involving long-lived $Ru(bpy')(DIP)_2^{2+}$ were obtained by tail fit of the exponential decay after the IRF.

Steady-state luminescence spectra of PS1, PS2 and PS3

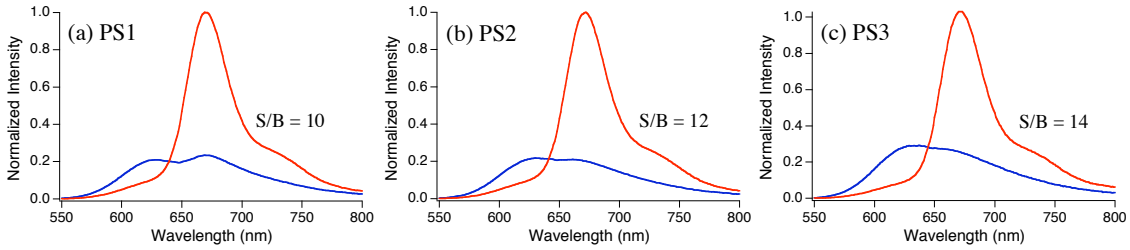

Figure S1. (a) PS1, (b) PS2, and (c) PS3 with (—) and without target (—). The S/B ratio seems to increase as the number of bases in the Cy5-probe decrease. The S/B ratio depends on the extent of the increase in the signal of Cy5 and the decrease in the signal of Ru(bpy')$(DIP)_2$. In buffer solution, most of the background fluorescence is due to non-specific Cy5 fluorescence. This fluorescence may be due to direct excitation of the Cy5-probe at the excitation wavelength of the Ru donor or to RET due to non-specific binding of Ru(bpy')$(DIP)_2^{2+}$ to DNA. Ru(bpy')$(DIP)_2^{2+}$ is known to have a high affinity for DNA, which can cause intermolecular interaction with a vicinal Cy5-probe. Figure S1 shows that this interaction might be less stable as the DNA sequence in the probe become shorter. This would decrease the fluorescence intensity of the Cy5-probe in the absence of target increasing the S/B ratio, consistently with the spectra in Figure S1.

Time decay analysis for the different PS

Legend

R = Ru(bpy')$(DIP)_2^{2+}$

R
= Ru-probe

nR
= Ru-probe sequence without Ru(bpy')$(DIP)_2^{2+}$

C = Cy5

C_1
= Cy5-probe1

C_2
= Cy5-probe2

C_3
= Cy5-probe3

nC_1
= Cy5-probe1 sequence without Cy5

nC_2
= Cy5-probe2 sequence without Cy5

nC_3
= Cy5-probe3 sequence without Cy5

Table S1. Lifetime data for different PS

Entry		$\tau_{exc.\ 460/em.\ 615}$, [a] ns	$\tau_{exc.\ 460/em.\ 667}$, [a,b] ns	$\tau_{exc.\ 659/em.\ 680}$, [a] ns (abundance, %)
1	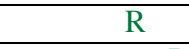	696	-	-
2	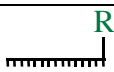	1780	-	-
3	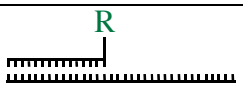	1780	-	-
4	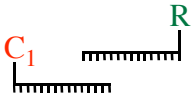	1790	-	1.1 (37) 2.0 (63)
5	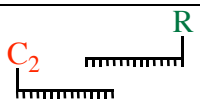	1730	-	1.1 (35) 2.1 (65)
6	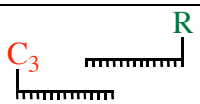	1770	-	0.9 (43) 1.8 (57)
7	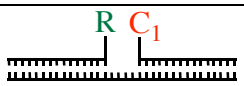	1620	1620 44	1.1 (34) 2.1 (66)
8	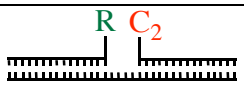	1600	1600 45	1.1 (28) 2.1 (72)
9	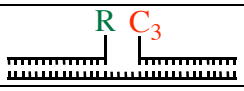	1680	1680 69	1.3 (33) 2.2 (67)
10	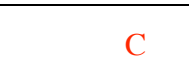	-	-	0.4 (21) 1.0 (79)
11		-	-	1.0 (35) 2.0 (64)
12		-	-	1.1 (40) 2.2 (60)
13		-	-	0.9 (48) 1.8 (52)
14	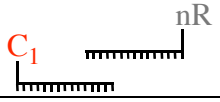	-	-	1.1 (41) 2.1 (59)
15	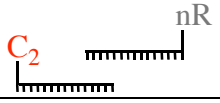	-	-	1.0 (31) 2.1 (69)
16	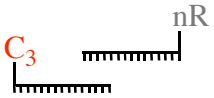	-	-	0.9 (44) 1.8 (56)
17	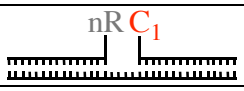	-	-	1.2 (42) 2.1 (58)
18	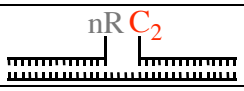	-	-	1.0 (36) 2.0 (64)

19	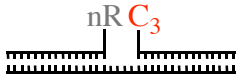	-	-	1.2 (37) 2.0 (63)
20		1780	-	-
21		1760	-	-
22		1750	-	-
23	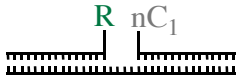	1930	-	-
24	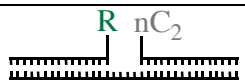	1850	-	-
25	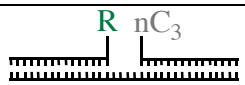	1790	-	-

[a] Uncertainty of ca. ±10%

[b] Tail exponential and biexponential fit starting after the decay of the IRF were used to extract lifetime parameters. Since the first moments of the transient can not be used in the fitting routine due to overlap with the IRF, a good portion of the contribution of the short-lived component is not taken into account, affecting the determination of accurate preexponential factors. For this reason, preexponential factors are not reported for the lifetimes determined for the RET process (Exc 460 nm, Em. 667 nm).

The luminescence lifetime of Ru(bpy')$(DIP)_2^{2+}$ in solution is 696 ns (Table S1, Entry 1). The linkage of the complex to the DNA produce an increase in the lifetime of the Ru(bpy')$(DIP)_2^{2+}$ to 1780 ns (Entry 2), probably by partially protecting it from quenching by molecular oxygen. Addition of target DNA to the Ru-probe does not change significantly the lifetime of the probe (Entry 3). However, the addition of the nC_1-probe, nC_2-probe, and nC_3-probe (the Cy5-probe sequences without the Cy5) in the presence of target increase the lifetimes to 1930 ns, 1850 ns, and 1790 ns, respectively (Entry 23-25). The decreasing lifetimes are probably caused by the decreasing chain length of the Cy5-probes, which decreases the distance from the Ru-probe. This suggests that the ruthenium complex does not interact strongly with the double stranded (dd) DNA formed when Ru-probe binds to target but it does interact with the dd DNA formed by Cy5-probe sequence and the target.

In contrast, the Cy5 fluorophore fits to a biexponential function with lifetime of 1.0 ns and 0.4 ns when free in solution and when excited at 659 nm (Entry 10) that virtually doubles when it is bound to the probe sequence (Entry 11-13). Addition of the Ru-probe, nR-probe (the Ru-probe without the Ru(bpy')$(DIP)_2^{2+}$) and the target sequence does not change significantly the lifetime of Cy5 (Entry 14-19).

The luminescence lifetimes of the Ru-probe with Cy5-probes (PS1, PS2, and PS3) free in solution (Entry 4-6), show values similar to that of just the Ru-probe in solution (Entry 2). Addition of target to PS1, PS2, and PS3 produces an increase in the observed fluorescence decay lifetime of Cy5 (667 nm) in the three PS (Entry 7-9), when excited at 460 nm. This decay lifetime is more than 20 times longer than the fluorescence of the probe excited directly (Entry 17-19) and it is due to the SF-RET from the ruthenium

complex to Cy5. Since the SF-RET is a slow process, the energy is transferred gradually causing a delay in the fluorescence emission. This fluorescence delay increases as the SF-RET rate constant decrease. Based on Förster's RET theory, the RET rate constant decreases as the distance between the RET pair increase.[6] It can be also noted from Table S1 that the delayed Cy5 lifetime (Exc. 460 nm, Em. 667 nm) increases as the Cy5-probes get separated from the Ru-probe from 44 ns to 45 ns to 69 ns when the number of nucleotides in between the probes increases from 5 to 6 to 10. A computer simulation using the program FRETview[7] (Figure S2) shows delayed fluorescence Cy5 lifetimes from 62 to 76 ns when the distance between the probes is between 28 to 29 Å, which is a reasonable estimation for the distance of the probes when PS3 is hybridized to target. The longer component (1.6-1.7 μs) observed exciting at 460 nm and monitoring at 667 nm (Entry 7-9), decays slightly faster than Ru-probe free in solution, and is observed also at $Ru(bpy')(DIP)_2^{2+}$ emission wavelength (615 nm) indicating that it corresponds to Ru-probe not bound to target.

(a) (b)

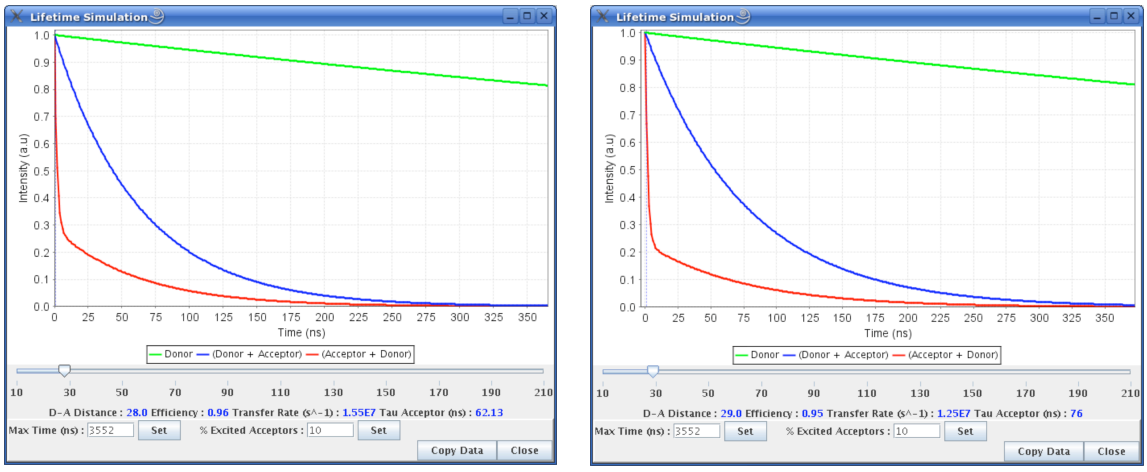

Figure S2. Screen shoot from the FRETView simulation of the RET components for PS3 (a) at a distance of 28 Å and (b) at a distance of 29 Å: — donor fluorescence in the absence of target, — donor fluorescence in the presence of target, — acceptor-delayed fluorescence in the presence of target. The donor decay lifetime in the presence of target (—) is not detected in our experimental transients since the RET process is over 95% efficient.

Determination of optimum time window for TRES experiments

$$\text{Optimization Ratio} = \frac{\dfrac{\text{Acceptor decay with Target}}{\text{Acceptor decay without Target}}}{\dfrac{\text{Donor decay with Target}}{\text{Donor decay without Target}}}$$

The optimization ratio has the purpose of helping to determine the time window for optimum S/B ratio. The numerator of the equation takes into account the increase in

the luminescence intensity of the acceptor when the target is added, whilst the denominator takes into account the reduction of the fluorescence of the donor in the presence of the target. The ratio of the increase in fluorescence of the acceptor and the decrease in the fluorescence of the donor at different times results in a curve where the maximum corresponds to the time window for optimum S/B ratio. For the TRES, we have chosen times slightly longer than the curve maximum in order to put some distance between the time window and the IRF, however this affect only slightly the S/B ratio. Figure S3 shows the fluorescence decay of PS3 and PS4 with target, together with the calculated optimization ratio curves.

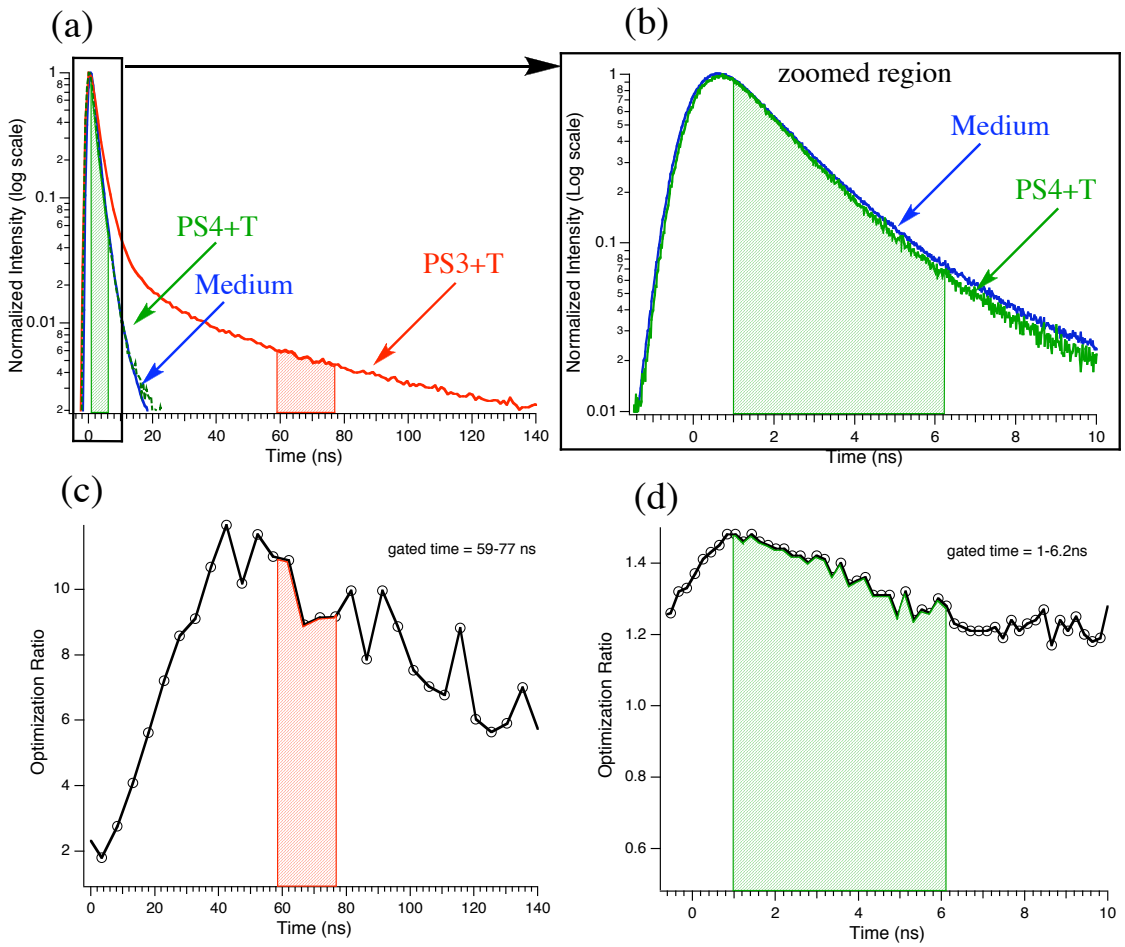

Figure S3. (a) Time decay of medium, PS3 in the presence of target, and PS4 in the presence of target (Exc. 460 nm, Em. 667 nm). (b) Detailed view of the 0-10 ns region of Figure S3a. (c) Optimization ratio curve for (c) PS3 (every point correspond to the average of 5 channel points) and (d) PS4 (every point correspond to an average of 10 channel points).

Sensitivity assessment to detect target DNA

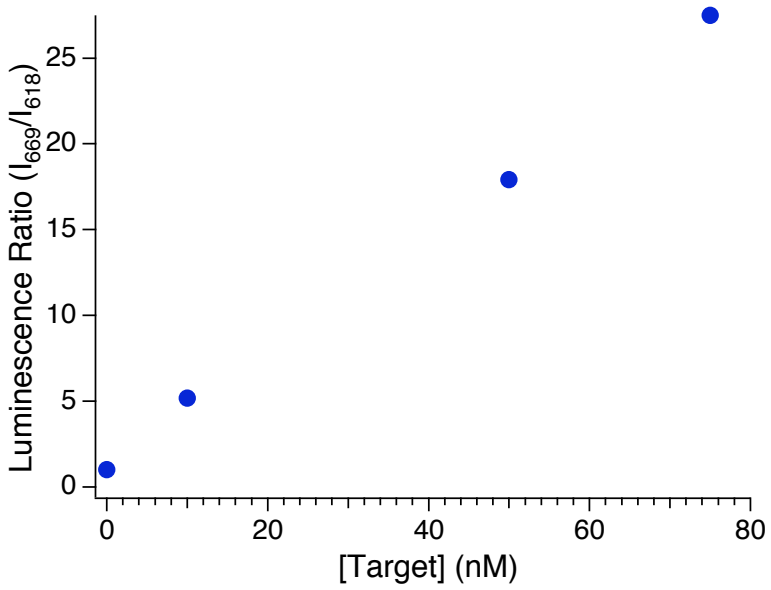

Figure S4. Ratio of the luminescence intensity of Cy5 (669 nm) and Ru (618 nm) after excitation of the binary probes (100 nm) at 440 nm in the absence and presence of different target concentrations.

To assess the sensitivity of the binary probe system, steady state fluorescence experiments were performed at different target DNA concentrations. Figure S4 shows a fairly linear increase of the luminescence ratio with the increase of target concentration. The figure also shows that a concentration of 10 nM can readily be detected with an ratiometric increase of 5 over the background fluorescence (in the absence of target).

References:

1. Martí, A. A.; Li, X.; Jockusch, S.; Li, Z.; Raveendra, B.; Kalachikov, S.; Russo, J. J.; Morozova, I.; Puthanveettil, S. V.; Ju, J.; Turro, N. J., *Nucleic Acids Res.* **2006**, *34*, (10), 3161 - 3168.
2. Sullivan, B. P.; Salmon, D. J.; Meyer, T. J., *Inorg. Chem.* **1978**, *17*, 3334–3341.
3. Della Ciana, L.; Hamachi, I.; Meyer, T. J., *J. Org. Chem.* **1989**, *54*, 1731-1735.
4. Holmlin, R. E.; Dandliker, P. J.; Barton, J. K., *Bioconjugate Chem.* **1999**, *10*, 1122-1130.
5. Martí, A. A.; Li, X.; Jockusch, S.; Stevens, N.; Li, Z.; Raveendra, B.; Kalachikov, S.; Morozova, I.; Russo, J. J.; Akins, D. L.; Ju, J.; Turro, N. J., *Tetrahedron* **2007**, *63*, 3591-3600.
6. Lakowicz, J. R., Principles of fluorescence spectroscopy. 2nd ed.; Kluwer Academic/Plenum Publishers: New York, 1999, p 368 - 394.
7. Stevens, N.; Dyer, J.; Martí, A. A.; Solomon, M.; Turro, N. J., *Photochem. Photobiol. Sci.* **2007**, doi: 10.1039/b702631e.